Theoretical investigation of bulk ordering and surface segregation in Ag-Pd and other isoelectornic alloys

A. V. Ruban,[1] S. I. Simak,[2] P. A. Korzhavyi,[1] and B. Johansson[1]
[1]*Applied Material Physics, Department of Materials Science and Engineering, Royal Institute of Technology, SE-100 44 Stockholm, Sweden*
[2]*Department of Physics, Chemistry and Biology, Linköping University, SE-581 83 Linköping, Sweden*
(Received 6 September 2006; published 23 February 2007)

Bulk ordering in Ag-Pd and other isoelectronic alloys is investigated theoretically by a number of first-principles techniques. The electronic structure and total energy have been calculated by the Green's function Korringa-Kohn-Rostocker and full-potential plane wave methods. The effective cluster interactions of the Ising-type Hamiltonian have been obtained by the screened generalized perturbation method. They reveal a complex concentration-dependent ordering behavior in these alloys due to band filling and Fermi surface effects. In particular we show that long-period superstructures are gradually stabilized by a great number of relatively weak long-range effective pair- and three-site interactions, which can be seen as "collective" effect. A similar complex concentration dependence is also found for surfaces of Ag-Pd alloys. The surface composition of the (111) and (100) surface of $Ag_{75}Pd_{25}$, $Ag_{50}Pd_{50}$, and $Ag_{33}Pd_{67}$ alloys have been then investigated by the surface Green's function technique and the screened generalized perturbation method for the effective interactions of the Ising-type Hamiltonian and the grand canonical Monte Carlo method for statistical thermodynamic simulations at finite temperatures. We compare our results with experimental data and other theoretical calculations.

DOI: 10.1103/PhysRevB.75.054113 PACS number(s): 64.75.+g, 64.90.+b, 68.35.Dv

I. INTRODUCTION

A classical Ising Hamiltonian is a main tool in statistical thermodynamic simulations of phase equilibria in alloys. It gives a simple, convenient and clear representation of the configuration energy of an alloy in terms of atomic distribution correlation functions and so-called effective cluster interactions.[1–3] It is commonly believed to be physically sound. However, this is far from obvious, since it is in fact quite a primitive phenomenological model without any firm physical ground, in spite of the fact that the cluster variables provide a complete and orthogonal basis for the expansion of the thermodynamic properties in terms of the corresponding effective interactions.[4] In fact the latter is only valid if the interactions are finite, which in its turn is entirely determined by the corresponding physical laws, which do not guarantee at all the existence of such a condition.

The point is that the effective interactions are expected to reproduce the energetics of *different* systems, i.e., systems having different electronic structure due to different arrangements of atoms on the lattice. So, if there is indeed a classical Hamiltonian, which can reproduce all the changes of a system, why do we need at all to solve the Schrödinger equation? On the other hand, if a classical description of the alloy configurational degrees of freedom by the Ising Hamiltonian is approximate, then how can one find an optimal set of interaction parameters giving the best possible classical Ising-type representation of a system, at least within a specific region of the configurational space?

The answer to this question is not clear at all, despite the fact that first-principles investigations of the phase equilibria in metallic alloys are becoming almost a routine exercise,[5] and moreover there have recently been made several attempts to solve this problem.[6–9] In this paper we do not answer this question either, however, we will demonstrate and argue along the line of Ref. 10, that the generalized perturbation method (GPM),[3,11,12] based on the coherent potential approximation (CPA), substantially simplifies the solution of this problem by providing a physically transparent picture of ordering, the knowledge of the most important interactions, and a set of effective interactions, which accurately reproduces the configurational energetics of the system. Moreover, we show that there are cases, where it is hardly possible to solve this problem without some preliminary knowledge of the effective interactions, given by the GPM or similar methods.[13,14]

The advantage of the GPM becomes obvious in the case of inhomogeneous systems and surfaces in particular. The main problem here is that the effective interactions become position-(layer-) dependent and thus their number grows sharply relative to that in the bulk. The structure inverse method (SIM) or Connolly-Williams method[15,16] has quite profound practical restrictions in this case, since a substantial number of supercells of a large size should be used in the first-principles calculations to get the corresponding effective interactions. Besides, the SIM severely suffers from a quite arbitrary choice of a restricted set of the basis clusters in the expansion and frequently from dubious implementations.

On the other hand, in the GPM all the interactions are obtained straightforwardly and relatively independently of the computational cost. In fact the GPM has been quite extensively used in the early days of the first-principles calculations of the surface concentration profiles.[17,18] However, it has been later recognized that (1) GPM cannot be used for calculations of the extensive properties (like on-site interactions, chemical potentials and segregation energies),[19] and (2) it should be supplemented by an additional screened Coulomb interaction term, taking care of the electrostatics.[20,21]

As has been recently demonstrated, the screened GPM (SGPM), which includes the corresponding screening correction, produces effective interactions yielding accurate configurational energetics in the bulk and as well as at the surface of metallic systems.[10,21,22]

In this paper we apply the SGPM to bulk and surface Ag-Pd alloys. On the one hand, this allows us to illustrate the above-mentioned points and, on the other hand, to learn something new about this system. There are several reasons to expect that the SGPM should be fairly accurate for Ag-Pd alloys. First of all, Ag and Pd are neighbors in the Periodic Table and therefore the CPA error cannot be large. Second, the size difference of Ag and Pd is comparatively small, so the relaxation effects are practically negligible in this system. This allows one to neglect these effects in thermodynamic consideration without losing important physics (we will include them, however, when they are needed for reaching a final verdict on stability issues).

According to the existing experimental information, Ag and Pd form continuous fcc solid solutions over the whole concentration range below the melting point.[23] Nevertheless, the first-principles calculations have predicted the existence of ordering tendencies in this system.[24–26] In particular, Müller and Zunger[25] have found three ground state structures: $L1_2$ for Ag_3Pd, $L1_1$ for AgPd, and the so-called $L1_1^+$ for $AgPd_3$, with transition temperatures 340, 320, and 270 K, respectively. These results are in agreement with those by Lu *et al.*[24] and Curtarolo *et al.*[26] for the Ag-Pd alloys, although Curtarolo *et al.*[26] have found the $L1_2$ structure to be just marginally stable compared to the DO_{22} structure for Ag_3Pd.

In this paper we study the ordering trends in Ag-Pd alloys. In order to have a more general picture we also investigate the ordering behavior in alloys isoelectronic to Ag-Pd: Cu-Pd, Au-Pd, Cu-Pt, Ag-Pt, and Au-Pt. We analyze the origin of the ordering trends in terms of the effective interactions. Finally we calculate the surface concentration profiles and chemical ordering for the (111) and (100) surfaces of $Ag_{75}Pd_{25}$, $Ag_{50}Pd_{50}$, and $Ag_{33}Pd_{67}$ alloys using effective interactions obtained by the SGPM and on-site interactions (surface segregation energies) from the corresponding surface Green's function calculations. The composition of the (111) and (100) surfaces of $Ag_{33}Pd_{67}$ has been recently obtained by means of the scanning tunneling microscopy (STM) experiments.[27] It has been established that the concentration of Pd atoms on the (111) surface varies in the range of 5%–11% for temperatures 720–920 K, while the (100) surface is entirely covered by Ag atoms. The STM is a unique technique, using which one can practically make direct observations of the surface structure, and therefore these data can be considered as reliable.

II. METHODOLOGY

A. Electronic structure and total energy calculations

Several different first-principles techniques have been used in this work. Most of the calculations have been done by the bulk and surface Green's function techniques in the framework of the Korringa-Kohn-Rostoker (KKR) method in the atomic sphere approximation (ASA)[28,29] combined with the CPA for treating random alloys as described in Refs. 30 and 31. We have also used the full potential projector augmented wave method (PAW)[32,33] implemented in the Vienna *ab initio* simulation package (VASP)[34,35] for the total energy calculations of ordered alloys. In the PAW calculations the required convergence has been reached for the energy cutoff of 313.5 eV and the integration over the Brillouin zone performed by means of the modified tetrahedron method with up to 4913 irreducible k points depending on the size and symmetry of the system.

All the KKR-ASA calculations have been done in the local density approximation (LDA)[36] with the Perdew-Wang parametrization for the exchange-correlation potential and energy.[37] The partial waves in the KKR-ASA calculations have been expanded up to $l_{\max}=3$ inside atomic spheres, while the multipole moments of the electron density have been determined up to $l_{\max}^M=6$ for the multipole moment correction to the Madelung potential and energy. Let us state again[21] that it is impossible to get correct ordering energetics in the KKR-ASA method without these multipole moment contributions. At the same time, the correct account of these contributions requires the knowledge of the states having higher moments, therefore at least f states should be included in the basis.[21]

The core states have been recalculated after each iteration. The number of k points for the Brillouin zone integration, performed by means of the Monkhorst-Pack scheme,[38] has been varied depending on the size and symmetry of the system and type of calculations in order to achieve the needed accuracy, and it has been especially high in the calculations of the energy difference of the long period superstructures (see below) and the long-range effective pair interactions.

The surface energy calculations have been done by employing a semi-infinite geometry with 9 and 12 surface layers for the (111) and (001) surfaces, respectively. The calculations of the GPM interactions for the first two surface layers in the case of alloy surfaces have been done by the bulk Green's function technique for slabs consisting of seven atomic and five vacuum layers for the (111) surface and six atomic and six vacuum layers for the (001) surface.

B. Screened Coulomb interactions

The electronic structure of random alloys have been obtained in the density-functional-theory-single-site KKR-ASA-CPA calculations with the on-site Coulomb screening potential, v_{scr}^i (Ref. 21) defined as

$$v_{\mathrm{scr}}^i = -e^2\alpha_{\mathrm{scr}}\frac{q_i}{S}, \tag{1}$$

where q_i is the net charge of the atomic sphere of the ith alloy component, S the Wigner-Seitz radius, and $\alpha_{\mathrm{scr}} \equiv \alpha_{\mathrm{scr}}(\mathbf{R}=0)$ the on-site screening constant. The latter has been determined from the screening charge around an "impurity" in an alloy,[20,21] which has been obtained in the locally self-consistent Green's function (LSGF) calculations[39,40] of 864-atom supercells modeling random $A_{75}B_{25}$ or $A_{50}B_{50}$ alloys.[41–43]

TABLE I. Effective charge transfer q_{eff} and screening constants, α_{scr} (**R**), on-site [**R**=(000)] and at the first six coordination shells in different alloys.

		$\alpha_{\text{scr}}(\mathbf{R})$						
Alloy	q_{eff}	**R**=(000)	(110)	(200)	(211)	(220)	(310)	(222)
$Ag_{75}Pd_{25}$	0.069	0.161	0.2141	0.0418	−0.0112	−0.0006	0.0064	0.0080
$Ag_{25}Pd_{75}$	0.035	0.138	0.2384	0.0233	−0.0341	−0.0404	0.0046	0.0134
$Ag_{75}Pt_{25}$	0.111	1.249	0.0540	−0.0271	−0.0017	−0.0020	−0.0033	−0.0002
$Ag_{25}Pt_{75}$	0.156	0.886	0.1062	−0.0052	−0.0020	0.0068	−0.0020	0.0134
$Au_{50}Pd_{50}$	0.180	0.656	0.1517	0.0072	−0.0108	−0.0105	−0.0001	0.0026
$Au_{25}Pd_{75}$	0.167	0.695	0.1463	0.0015	−0.0131	−0.0128	−0.0007	0.0031
$Au_{75}Pt_{25}$	0.010	−2.513						
$Au_{25}Pt_{75}$	0.015	1.751						
$Cu_{50}Pd_{50}$	0.309	0.815	0.1149	−0.0057	−0.0073	−0.0069	−0.0015	0.005
$Cu_{50}Pt_{50}$	0.572	0.776	0.1233	−0.0021	−0.0072	−0.0040	−0.0006	0.0013
SS-LSGF		0.605	0.1569	−0.0017	−0.0158	−0.0098	−0.0005	0.0015

The screening charge has also been used to determine the intersite screening constants, $\alpha_{\text{scr}}(\mathbf{R})$, needed in the calculations of the electrostatic part of the SGPM effective pair interactions,[20,21] i.e., the screened intersite Coulomb interactions, which in the case of a binary *A*-*B* alloy can be defined as

$$V^{\text{scr}}(\mathbf{R}) = e^2 \alpha_{\text{scr}}(\mathbf{R}) \frac{q_{\text{eff}}^2}{S}, \tag{2}$$

where $q_{\text{eff}}=q_A-q_B$ is the effective charge transfer in the case of a binary alloy. The whole SGPM interaction is then

$$V_i \equiv V(\mathbf{R}) = V^{\text{one-}el}(\mathbf{R}) + V^{\text{scr}}(\mathbf{R}), \tag{3}$$

where V_i is the SGPM interactions at the *i*th coordination shell, given by set of vectors **R**, and $V^{\text{one-el}}(\mathbf{R})$ the one-electron contribution to the SGPM interaction.[3,20,21]

In Table I we present the results for the on-site [**R**=(000)] and intersite screening constants for Ag-Pd and alloys isoelectronic to Ag-Pd. In the last line of the table we show the screening constants obtained in the LSGF calculations with a single-site local interaction zone (SS-LSGF). They do not practically depend on the system under consideration and can be considered as universal.[20] Only the inclusion of the local environment and polarization effects (through the multipole moments) makes the screening system specific.

One can see that these effects lead to huge variations of the screening constants including a quite strong concentration dependence. The largest deviations of the screening constants from SS-LSGF values are found in the systems with the lowest effective charge transfer, which are the Au-Pt alloys. In this case the formalism, developed for the screening of monopole net charges of the atomic spheres, actually breaks down, since the dominant contribution to the screening comes from monopole-multipole electrostatic interactions. The on-site screening constants for the Au-Pt alloy cannot be used in the usual single-site-DFT-CPA calculations, although they still satisfy the criteria of being the average on-site screening constants in the supercell of a random alloy: $\langle v^i_{\text{Mad}}\rangle = e^2\alpha_{\text{scr}}\langle q_i\rangle/S$, where $\langle v^i_{\text{Mad}}\rangle$ and $\langle q_i\rangle$ are the average Madelung potential and net charge of the *i*th component.

In the Ag-Pd alloys the effective charge transfer is also quite small (see q_{eff} Table I), and this leads to the anomalously low values of the on-site screening constant, α_{scr}. We have used these values anyway in our single-site-DFT-CPA calculations, since the error in the contribution to the one-electron potential should be small. Let us also notice a pronounced sensitivity of the screening constants to the alloy composition in alloys with small charge transfer effects. Such a sensitivity originates from the concentration dependence of the screening properties of alloys, when band structure changes from an active *d*-band in Pd(Pt)-rich compositions to almost inert, impuritylike, in Ag (Cu,Au)-rich alloys (see discussion below) indicating a quite complex concentration-dependent character of bonding in these systems.

C. Statistical thermodynamic simulations

The atomic configurational energy of Ag-Pd alloys has been mapped onto an Ising-type Hamiltonian with concentration-dependent effective cluster interactions, which, when generalized for surfaces, can be written in the following way:

$$H = \sum_{i\lambda} \tilde{V}^{(1)}_{\lambda}\sigma_{i\lambda} + \frac{1}{2}\sum_{i\lambda;j\lambda'} \tilde{V}^{(2)}_{\lambda\lambda';p(ij)}\sigma_{i\lambda}\sigma_{j\lambda'} + \frac{1}{3}\sum_{i\lambda;j\lambda';k\lambda''} \tilde{V}^{(3)}_{\lambda\lambda'\lambda'';t(ijk)}\sigma_{i\lambda}\sigma_{j\lambda'}\sigma_{k\lambda''} + \cdots, \tag{4}$$

where we have used spin-variables $\sigma_{i\lambda}$, which take on values 1 if site *i* in the λ layer is occupied by Ag, and −1 if it is occupied by Pd. Here $\tilde{V}^{(1)}_{\lambda}$ is the on-site interactions in the λth layer; $\tilde{V}^{(2)}_{\lambda\lambda';p(ij)}$ the effective pair interaction of type *p*

between λ and λ′ layers; and $\tilde{V}^{(3)}_{\lambda\lambda'\lambda'';t(ijk)}$ the 3-site interaction of type t. Here we have used tilde to distinguish spin-variable interactions from usual GPM interactions, $V^{(n)}$, defined in the concentration-variable basis, $c_i=1/2(\sigma_i+1)$. They are related to each other as $V^{(n)}=2^n\tilde{V}^{(n)}$.

As has been mentioned above, we use the concentration-dependent form of all the effective interactions, but on-site. The latter has been determined for each layer from the total energy of the equiatomic homogeneous random alloy in the surface region on top of the corresponding bulk alloy $E^{\text{tot}}\{(Ag_{50}Pd_{50})_{\text{surface}}/(Ag_cPd_{1-c})_{\text{bulk}}\}$, as

$$V^{(1)}_{\lambda}=\frac{\partial E^{\text{tot}}}{\partial\sigma_{\lambda}}, \tag{5}$$

and normalized to have $V^{(1)}_{\lambda}=0$ for the deep bulklike layers.

The pair and multisite interactions in Eq. (4) depend in fact on a particular concentration profile by definition.[17,18] As will be shown below, the effective interactions in AgPd exhibit concentration dependence. Therefore their values have been redetermined in the Monte Carlo simulations following the changes of the corresponding concentration profile.

The Monte Carlo simulations, based on the Metropolis algorithm,[44] for bulk alloys have been performed for a simulation box containing 6912 ($12\times12\times12\times4$) atoms. In the case of alloy surfaces we have used the direct exchange Monte Carlo (DEMC) method,[45] which is a grand canonical ensemble technique directly simulating the exchange of atoms between the bulk and the surface region. The size of the simulation box for surface calculations was 24×24 in the planes parallel to the surface and a thickness of 24 layers.

III. EFFECTIVE PAIR INTERACTIONS IN Ag-Pd

The change of ordering behavior in Ag-Pd alloys with Pd concentration, found by Müller and Zunger,[25] from a dominating $\mathbf{k}_s=2\pi/a(100)$ superstructure vector in Ag-rich alloys to $\mathbf{k}_s=\pi/a(111)$ at the equiatomic alloy composition and in Pd-rich alloys, is, of course, not something completely unexpected. A similar behavior has also been observed experimentally in the isoelectronic Cu-Pd and Cu-Pt alloys.[46,47] On the other hand, it is also well known that the (001)-type of ordering in the Cu-rich Cu-Pd alloys is accompanied by the formation of the so-called long-period antiphase boundary structures or simply long-period superstructures (LPS) along the [001] direction.

The latter are formed by periodic antiphase boundaries along a (001) plane. If the distance between the boundaries is aM, the LPS has a new periodicity $2aM$ along the [001] direction, and they can be called LPS M. In the neutron diffraction experiments for random alloys (above the ordering transition temperature) this type of ordering is seen as a formation of an additional diffuse scattering peak at $\mathbf{q}_m=2\pi/a(10\frac{1}{2M})$.[3] The position of $\mathbf{q}_m$ in general depends on the alloy composition and temperature. Although the concentration dependence is usually connected with Fermi surface nesting,[13,48–50] the origin of the temperature effect is under discussion.[51–53]

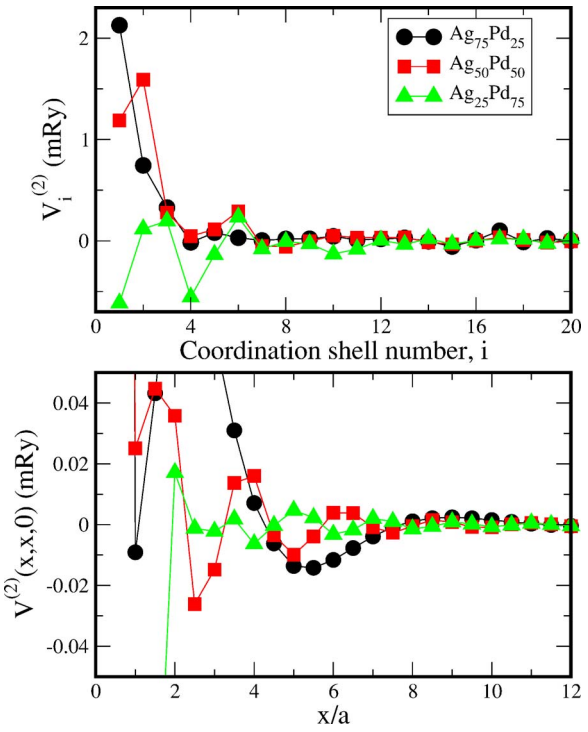

FIG. 1. (Color online) SGPM effective pair interactions in $Ag_{75}Pd_{25}$, $Ag_{50}Pd_{50}$, and $Ag_{25}Pd_{75}$ ploted as a function of interatomic distance, scaled by the lattice parameter, a.

As has been demonstrated in Ref. 10, the effective pair SGPM interactions are long-range and they exhibit a quite strong concentration dependence, reflected, for instance, in the concentration-dependent Friedel-type modulations along the closed-packed [110] direction. The three-site interactions are also relatively strong and long range, at least in the Ag-rich alloys. Therefore we have calculated the effective pair interactions in the bulk Ag-Pd alloys at the first 300 coordination shells, which span a distance of 8.48 units of the lattice spacing. We find that the behavior of the pair interactions in Ag-Pd alloys is very similar to that in Cu-Pd: They are very long-range and strongly concentration dependent.

This can be seen in Fig. 1, where we show the effective pair interactions at the first 20 coordination shells for three alloy compositions: $Ag_{75}Pd_{25}$, $Ag_{50}Pd_{50}$, and $Ag_{25}Pd_{75}$ (upper panel) as well as the effective pair interactions along the closed packed [110] direction (lower panel). In the latter case one can notice a substantial change with concentration of the Friedel-type modulation of the effective pair interactions. This is exactly what has in fact been observed in the case of CuPd system in Ref. 10. Let us notice that there are more than 280 coordination shells up to $\mathbf{R}=a(6,6,0)$ in total. Of course, only part of them should be considered in the energetics of ordering. However, the existence of so long-range and non-negligible interactions clearly demonstrates the practical problem of treating such systems even with the classical Ising-type Hamiltonian.

The change of the ordering behavior with concentration can be clearly seen in the Fourier transform of the effective pair interactions, $V(\mathbf{q})$, presented in Fig. 2. Here we show $V(\mathbf{q})$ in two (001) planes of the reciprocal space: one at q_z

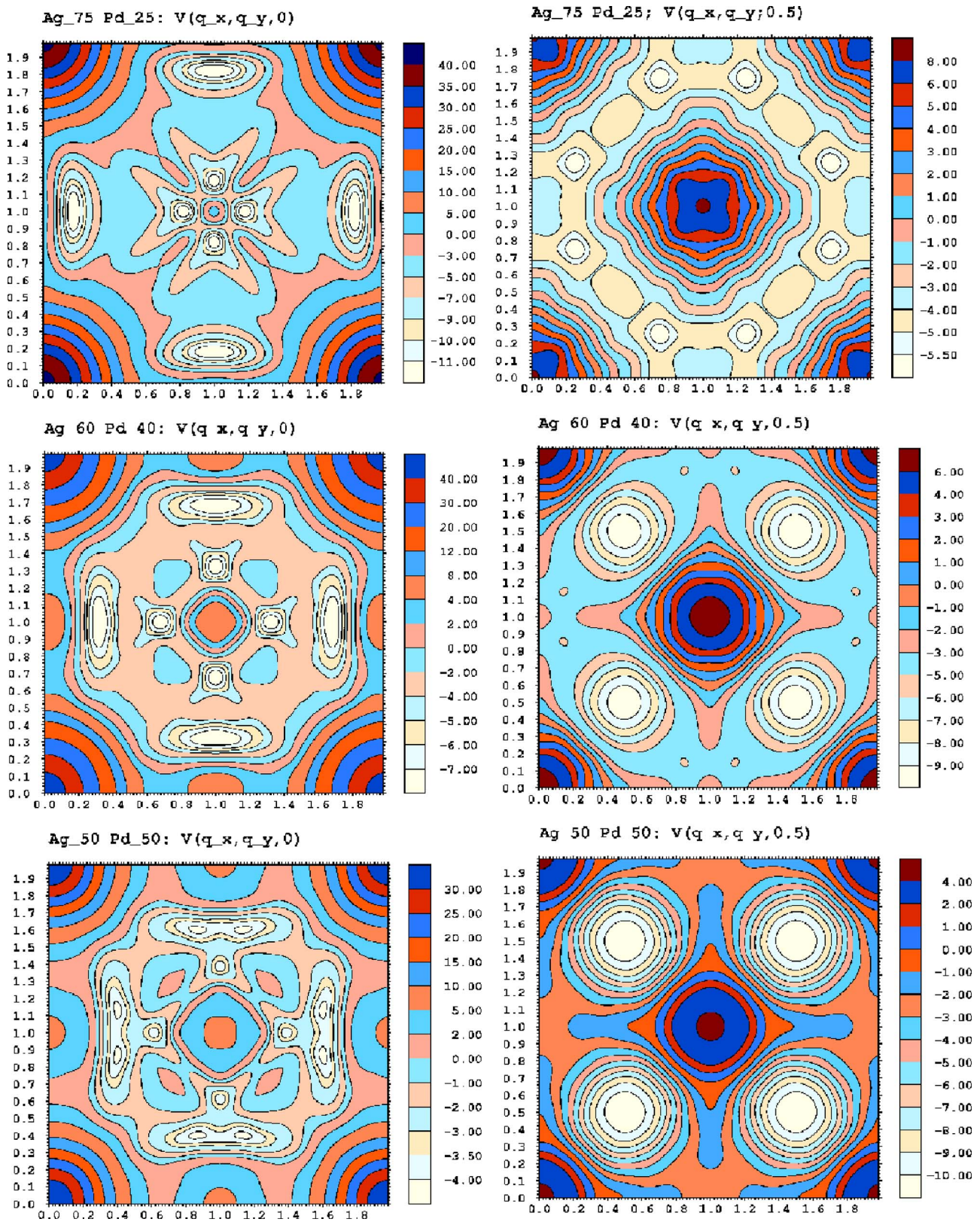

FIG. 2. (Color online) Fourier transform of pair interactions in $Ag_{75}Pd_{25}$ (top panel), $Ag_{60}Pd_{40}$ (middle panel), and $Ag_{50}Pd_{50}$ (bottom panel) in (001) plane at $q_z=0$ (on the left-hand side) and $q_z=\pi/a$ (on the right-hand side).

$=0$ (on the left-hand side) and the other one at $q_z=\pi/a$ (on the right-hand side). For the $Ag_{75}Pd_{25}$ alloy the minimum of $V(\mathbf{q})$ is approximately at $\mathbf{q}_m \approx 2\pi/a(1,0.18,0.0)$. The value of the local minima in the $q_z=\pi/a$ plane is much higher. This means that the formation of LPS3 $\left(0.18 \approx \frac{1}{2.3}\right)$ in the $Ag_{75}Pd_{25}$ alloy should be expected at low temperature. This

is, of course, very similar to the case of Cu-rich Cu-Pd and Cu-Pt alloys.

The behavior of $V(\mathbf{q})$ changes quite rapidly with Pd concentration and already for $Ag_{60}Pd_{40}$ one can observe a crossover from the $L1_2$-LPS-type of ordering to the $L1_1$-type with a superstructure vector $\mathbf{q}=2\pi/a(\frac{1}{2}\frac{1}{2}\frac{1}{2})$. At the equiatomic alloy composition the local minimum along $(1,q_y,0.0)$ (Γ-X direction of the Brillouin zone) disappears completely and the global minimum is at the L point, $\mathbf{q}=2\pi/a(\frac{1}{2}\frac{1}{2}\frac{1}{2})$. The evolution of the ordering behavior with Pd concentration in Ag-Pd alloys, presented in Fig. 2, is very similar to the one in Cu-Pd and Cu-Pt found in diffuse scattering experiments by Saha *et al.*[46,47]

Qualitatively this picture remains unchanged after the inclusion of multisite interactions, and in particular 3-site and 4-site interactions, which basically only modify the values of the ordering energies. Nevertheless, we should point out that (like in the case of the Cu-Pd alloys[10]) these interactions are quite long-range and not negligible despite their relatively small individual values. In the present work we have included 81 3-site interactions, which comprise of all the 3-site interactions up to the seventh coordination shell and a set of more distant interactions along the closed-packed direction, which are usually quite substantial in practically all the systems. We have also included 26 4-site interactions, which comprise all the 4-site interactions up to the fourth coordination shell and some additional more long-range interactions. However, in contrast to the 3-site interactions, they contribute very little to the energetics of ordering in this system.

IV. ORDERING IN Ag-Pd AND ISOELECTRONIC ALLOYS

A close similarity of the ordering behavior in Ag-Pd with Cu-Pd system is, of course, quite expected since Ag and Cu belong to the same group of the Periodic Table. At the same time other isoelectronic alloys, like, for instance, Ag-Pt, show rather different pattern of ordering and alloying.[54,55] The origin of similarities and differences in the same type of alloys is interesting, and therefore we investigate this problem here on the basis of the SGPM and total energy calculations of the following systems: Cu-Pd, Au-Pd, Cu-Pt, Ag-Pt, and Au-Pt.

Since we are mainly interested in finding qualitative trends, we, first, omit the problem of lattice relaxation effects, which is important in the Cu-Pd and Cu-Pt systems only for *quantitative* considerations, and, second, ignore the problem of finding the equilibrium lattice spacing, enthalpies of formation and theoretical ground state structures. In fact, all our KKR-ASA and SPGM calculations have been performed for fixed Wigner-Seits radii: $S_{WS}=2.98$ a.u. ($a=4.035$ Å) for Ag(Au)-Pd(Pt) alloys in the whole concentration range, and $S_{WS}=2.75$, 2.79, and 2.83 a.u. ($a=3.734$, 3.778, and 3.832 Å) in the case of $Cu_3Pd(Pt)$, CuPd(Pt) and $CuPd(Pt)_3$ alloys, respectively. Below we will demonstrate that the type of ordering is insensitive to the lattice spacing. This fact has also been established by Sluiter *et al.*[55] for Au-Pd alloys.

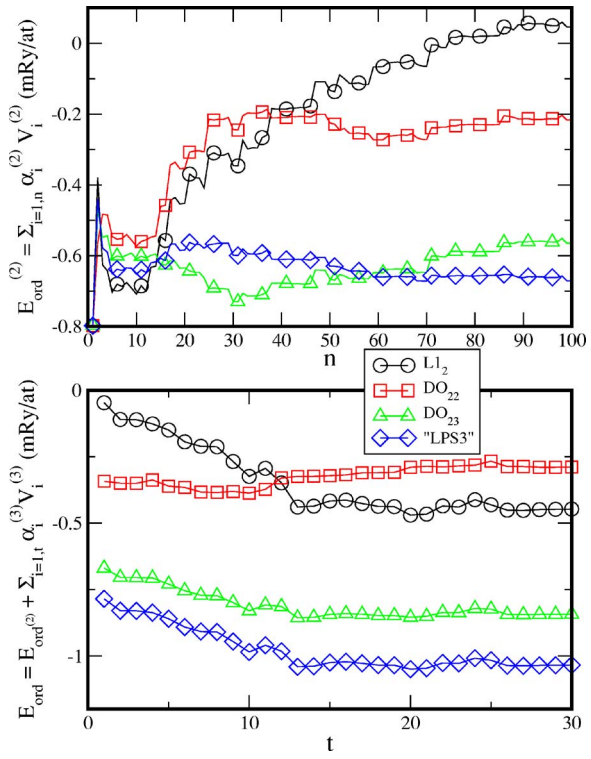

FIG. 3. (Color online) The ordering energies of the $L1_2$-, DO_{22}-, DO_{23}-, and LPS3-Ag_3Pd from the SGPM 2-site interactions (top panel) and 3-site interactions (lower panel), as a function of the number of interactions taken in the corresponding summation.

In Table II we present the energies of several ordered structures, relevant for our consideration, obtained by different methods. The energies are shown relative to that of the $L1_2$ structure in order to simplify the comparison. The agreement between all the direct first-principles calculations is very good, despite the fact the data from the literature are in fact the differences between the *enthalpies of formation of the relaxed* structures. It is obvious that lattice relaxations are negligible for Ag(Au)-Pd(Pt) alloys. The important point here is that the KKR-ASA method with the multipole moment correction for the electrostatic energy and potential [KKR-ASA(+M)] yields very accurate results for the *configurational energetics on a fixed lattice*. Therefore one may expect that the SGPM interactions calculated by this method can reproduce accurately the configurational energies.

Indeed, the results presented in Table II show that the SGPM interactions yield the ordering energies in very good agreement with the direct total energy calculations, except for two cases: There is a quite big error for the $V1$ structure in the case of Cu_3Pd and Cu_3Pt. We believe that the problem in these two cases originates from strong multipole-moment electrostatic interactions in the $V1$ structure due to the absence of the inversion symmetry on some Cu sites.

It should also be mentioned that by definition the GPM interactions are those which are relevant for the configurational energetics close to the *random state*, in which they are derived. In other words, there is no reason to expect in general, that they can reproduce exactly the energetics of ordered structures, whose electronic structure is substantially

TABLE II. The energies (in mRy/atom) of A_3B alloys relative to the energy of the $L1_2$ structure.

Structure	Cu_3Pd	Ag_3Pd	Au_3Pd	Cu_3Pt	Ag_3Pt	Au_3Pt	Method
DO_{22}	0.76	0.01	−0.36	1.36	0.48	0.09	KKR-ASA(+M)
(LPS1)	1.06	0.37	−0.26	1.26	0.62	0.75	SGPM
		0.03	−0.32				PAW
		0.04[a]	−0.3[c], −0.4[d]		0.39[c]		Others
DO_{23}	0.05	−0.23	−0.55	0.27	−0.06	−0.58	KKR-ASA(+M)
(LPS2)	0.01	−0.29	−0.64	−0.03	−0.32	0.0	SGPM
		−0.25	−0.55				PAW
			−0.60[d]				Others
LPS3	−0.22	−0.40	−0.56	−0.07	−0.26	−0.63	KKR-ASA(+M)
	−0.28	−0.52	−0.58	−0.26	−0.52	0.03	SGPM
		−0.43	−0.56				PAW
$L1_1^+$	2.57	0.41	1.25	3.24	−1.59	−0.92	KKR-ASA(+M)
	2.61	0.29	1.06	3.25	−1.55	−1.51	SGPM
			1.18[d]		−1.55[c]		Others
$V1$	5.42	1.34	3.38	6.66	−3.08	−1.92	KKR-ASA(+M)
	7.22	0.52	3.19	11.52	−1.77	−2.49	SGPM
		1.20[b]	3.16[d]		−2.27[c]		Others

[a]Reference 26.
[b]Reference 25.
[c]Reference 55.
[d]Reference 8.

different from that of the random alloy. Besides, there can be structure-specific contributions to the total energy, which originate from the actual symmetry of the ordered alloy, like, for instance, electronic structure effects associated with long-range order found by Johnson *et al.*[56] However the latter does not seem to be a problem in Ag-Pd alloys.

A. Trends in the ordering behavior

It is clear from Table II that all these alloys exhibit exactly the same trend of the stabilization of the LPS based on the $L1_2$ structure (let us notice, that the DO_{22} and DO_{23} structures can be considered as LPS1 and LPS2, respectively, while the $L1_2$ structure as LPS∞). The LPS3 is the most stable in the sequence of increasing value of M (the LPS4 is less stable, than LPS3, in all the cases).[57] The difference appears when we compare the relative stability of the LPS with so-called $L1_1^+$ and $V1$ structures.[24,25] One can easily identify two elements responsible for the differences in the ordering behavior: Cu (versus Ag and Au) and Pt (versus Pd).

It is interesting to notice that although the stabilization of the LPS in the Cu_3Pd is quite well known, it has never been predicted theoretically in the Ag_3Pd, and only recently the stabilization of the DO_{23} structure in Au_3Pd has been found in the *ab initio* calculations of Barabash *et al.*[8] The latest theoretical works on these systems by Müller and Zunger[25] as well as by Sluiter *et al.*,[55] which are based on the SIM for the enthalpies formation, have completely failed in this respect. Barabash *et al.*[8] have included the DO_{22} and DO_{23} structures in the set for the SIM, therefore it is rather *an observation*, than *a prediction*. The reason, why the formation of the LPS is so difficult to predict on the basis of the SIM, unless the corresponding structures are included in the calculations, is the Fermi-surface nesting nature of the stabilization of these structures,[13,48–50] which in terms of the Ising Hamiltonian is driven by the long-range effective interactions.

This point is demonstrated in Fig. 3, where the ordering energy of the $L1_2$, DO_{22}, DO_{23}, and LPS3 is plotted as a function of the number of pair and three-site interactions included in the corresponding summation. The LPS3 in the Ag_3Pd becomes stable only beyond the 70th coordination shell of the effective pair interactions (top panel of the figure). It is worth noticing that also the multisite GPM interactions cannot be neglected.

In the lower panel of the figure we show the contribution to the ordering energy from 3-site interactions (the initial energy is the ordering energy obtained from all the pair interactions up to the 140th coordination shell). Again, like in the case of Cu_3Pd, we find that although the individual contributions from 3-site interactions are relatively small, they accumulate a substantial contribution to the ordering energy. That is, this is a *collective* effect, which, as has been already mentioned, makes even the classical Ising-type consideration cumbersome. Now, if we also take into consideration the nonlinear concentration dependence of all these interactions, as pair, as well as multisite, it becomes clear that in the SIM

TABLE III. The energies (in mRy/atom) of AB alloys relative to the energy of the $L1_0$ structure.

Structure	CuPd	AgPd	AuPd	CuPt	AgPt	AuPt	Method
CH ("40")	−0.1	−0.7	−0.6	1.2	0.9	0.3	KKR-ASA(+M)
	−0.2	−0.9	−0.4	2.9	1.7	1.0	SGPM
			−1.0[b], −0.78[c]		0.2[c]		Others
$L1_1$	0.2	−1.7	1.3	−3.6	−7.9	−4.0	KKR-ASA(+M)
	−1.5	−1.9	1.9	−0.2	−5.6	−2.5	SGPM
		−1.6[a]	1.2[b], 1.4[c]	−2.1	−7.5		Others

[a]Reference 25.
[b]Reference 58.
[c]Reference 55.
[d]Reference 8.

approach,[8,25,55] where the cluster interactions are obtained from a relatively small number of structures with a small unit cell, there are simply no practical means to get the necessary information about plenty of so long-range effective interactions.

Let us note that the situation with the SIM becomes much worse, when the *enthalpies* of formation of alloys over the whole concentration range[8,25,55] are used for mapping onto on Ising-type Hamiltonian. In this case the higher order (multisite) cluster interactions should take care of the corresponding concentration, volume and relaxation dependencies of the lower order interactions. This means that the number and the *order* of the concentration-volume-relaxation independent interactions should be much greater than considered in Fig. 3. The restrictions of the SIM imposed by both the arbitrarily truncated basis of interactions and by the specific finite set of structures used in the first-principles calculations allow predicting only the ordered structures "adaptive" to this set. If the LPS are not included in the basis, as in the case of Ag-Pd alloys, they will be missed no matter which algorithm is used to obtain the cluster interactions. Of course, if the information about the competing LPS is known, the corresponding structures can be directly included in the basis,[6] which solves the problem in this particular case, but not in general.

In Table III we present the energies of equiatomic $L1_1$ and CH or "40" (the definition of this structure can be found in Ref. 24) ordered structures relative to that of the $L1_0$. One may notice that now the Ag-Pd and Au-Pd alloys exhibit different types of ordering, although they behave very simi-

TABLE IV. The energies (in mRy/atom) of AB_3 alloys relative to the energy of the $L1_2$ structure.

Structure	$CuPd_3$	$AgPd_3$	$AuPd_3$	$CuPt_3$	$AgPt_3$	$AuPt_3$	Method
DO_{22}	0.89	0.80	0.15	2.97	2.12	0.95	KKR-ASA(+M)
	1.73	0.78	0.04	4.03	2.4	0.75	SGPM
		0.03[a]	−0.07[b], 0.18[c]		0.64[b]		Others
DO_{23}	0.50	0.53	0.18	0.21	0.41	0.18	KKR-ASA(+M)
	0.80	0.75	0.05	1.07	0.65	0.00	SGPM
			0.23[c]				Others
LPS	30.31	0.30	0.12	0.53	0.51	0.27	KKR-ASA(+M)
	0.52	0.69	0.02	0.79	0.47	0.03	SGPM
$L1_1^+$	0.80	−0.40	1.19	0.66	−2.78	−0.96	KKR-ASA(+M)
	1.26	0.04	0.93	0.15	−2.63	−1.51	SGPM
		−0.34					PAW
		−0.22[a]	0.73[b]		−2.41[b]		Others
$V1$	3.79	0.56	2.91	7.71	−1.37	−1.20	KKR-ASA(+M)
	4.81	0.30	2.40	8.82	−2.56	−2.49	SGPM
		0.62					PAW
		0.08[a]	3.45[b]		−3.12[b]		Others

[a]Reference 25.
[b]Reference 55.
[c]Reference 8.

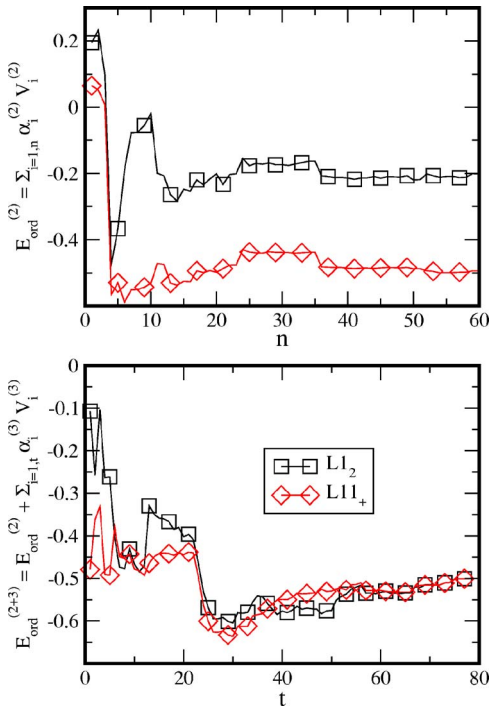

FIG. 4. (Color online) The ordering energies of the $L1_2$- and $L1_1^+$-$AgPd_3$ from the SGPM 2-site interactions (upper panel) and 3-site interactions (lower panel), as a function of the number of interactions taken in the corresponding summation.

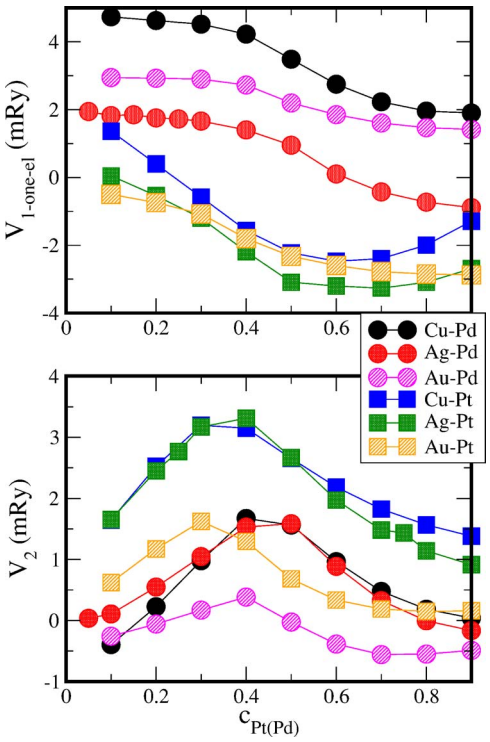

FIG. 5. (Color online) One-electron part of the GPM effective interaction at the first coordination shell (top panel) and the SGPM interaction at the second coordination shell (bottom panel).

larly in the case of Ag_3Pd and Au_3Pd alloys. Surprisingly this is not the case for the Pt alloys. All of them seem to have similar ordering trends: They prefer to form the $L1_1$ ordered structure on the fcc lattice. One can also notice that the SGPM interactions produce an error of the order of 1–3 mRy for the ordering energy of the $L1_1$ phase, which has much lower symmetry than the other phases considered here. Therefore there should be an additional structure-specific contribution to the total energy from the multipole-moment electrostatic interactions, unaccounted for by the SGPM.

Finally, Table IV shows the energies of $Cu(Ag,Au)Pd(Pt)_3$ ordered alloys relative to the energy of the $L1_2$ structure. One can see that the formation of the LPS is no longer favorable. At the same time the $L1_1^+$ structure becomes stable in $AgPd_3$ and $AgPt_3$. This result has been predicted by Müller and Zunger[25] for $AgPd_3$, while for $AgPt_3$ it is at variance with the recent calculations by Sluiter *et al.*[55] The origin of this discrepancy is unknown. However, this is not important since none of those structures is stable: This alloy should undergo phase separation.[55]

The SGPM interactions do not predict correctly the stable structure of $AgPd_3$. However, it is worth noticing that the energy balance between the $L1_2$ and $L1_1^+$ structures is quite delicate, and any inaccuracy can affect the result. For instance, the $L1_1^+$ structure stabilizes with Pd concentration: The SGPM interactions obtained for $Ag_{22}Pd_{78}$ reverse the stability in favor of the $L1_1^+$ structure. In Fig. 4 we demonstrate the nontrivial behavior of the $L1_1^+$-$L1_2$ energy difference as a function of the number of the pair- and 3-site SGPM interactions (for the $Ag_{25}Pd_{75}$ alloy composition). It is interesting to notice, that the contributions from the pair- and 3-site interactions to the energy difference of the $L1_1^+$ and $L1_2$ structures are almost the same but have the opposite sign, and while the pair interactions stabilize the $L1_1^+$ phase, the 3-site interactions stabilize the $L1_2$ structure (4-site interactions give a very little contribution to the energy of both phases).

V. ORIGIN OF ORDERING TRENDS

A. Nearest neighbor and next-nearest neighbor effective pair interactions

As we have seen above, the Ag-Pd-isoelectronic exhibit substantial variation of ordering behavior with alloy composition. We have also seen that the ordering energies are complicated functions of pair and multisite interactions (Fig. 3). Nevertheless the results presented above (apart from the formation of the LPS, which can be viewed as modulated $L1_2$ structures) can be qualitatively understood in terms of the effecitve pair interactions just at the first two coordination shells. These are the strongest interactions and therefore their contribution to the ordering energy is dominating, at least on a qualitative level.

The results for these two interactions are presented in Fig. 5. In order to simplify the comparison we present only the one-electron part of the SGPM interactions at the first coordination shell, $V_1^{\text{one-el}}$. In fact it is dominating in all the systems due to small effective charge transfer, q_{eff}, except for Cu-Pd and Cu-Pt (we will discuss the electrostatic contribution in Cu-Pt alloys later). At the same time, we consider the

total SGPM interaction at the second coordination shell, V_2, since the electrostatic term gives a very small contribution even in the case of Cu-Pd and Cu-Pd systems due to a small value of the corresponding screening constant, $\alpha_{scr}(200)$ (see Table I).

One can see that the change of both interactions with concentration is substantial and nonlinear (the latter may give a hint about the order of multisite interactions, which should be kept in the concentration-independent cluster expansion, needed to account for these concentration dependencies). In general the concentration dependencies of the interactions are very similar for all the alloys: An almost monotonic decrease of V_1 and a pronounced maximum of V_2 in the range of 30–40 at. % of Pt and 40–50 at. % of Pd. The similarity is especially striking for V_2 in the CuPd-AgPd and CuPt-AgPt systems.

At the same time it is easy to identify two elements, namely Pt and Au, which introduce distinctive differences in the concentration dependencies. First of all, the behavior of V_1 in Pd alloys is different from that in Pt alloys: while V_1 starts decreasing almost immediately with Pt concentration, there is a plateaulike feature in Pd alloys up to about 40 at. % of Pd. One can also see, that the substitution of Cu or Ag by Au also leads to different behavior in both cases: Au-Pd and Au-Pt look more similar to each other than to their Cu or Ag counterparts. One can speculate, that in the case of Au the difference originates from the well-known relativistic shift of the Au *s*-band, leading to an increase of its "nobility."[59] The difference between Pd and Pt can probably also be partly attributed to relativistic effects.[58] However, these are metals with an open *d*-shell and therefore the behavior of *d*-states, i.e., the position and width of the *d*-band, should play an important role.

B. Pd-Pd and Pt-Pt *d*-band mediated interactions

To clarify the role of the *d*-electrons in ordering behavior, let us note that an effective pair interaction characterizes the preference of the atoms of the same type to be at the corresponding coordination shell, which is phenomenologically expressed for an *A*-*B* alloys as $V=v^{AA}+v^{BB}-2v^{AB}$, where v^{XY} is the interatomic potential between *X* and *Y* atoms. In the systems under consideration there are three different type of interatomic interactions: between noble metals (Cu,Ag,Au), between transition metals (Pd,Pt), and between noble and transition metals. Although it is impossible to find the leading pair interatomic potentials in general, it is most likely that at the nearest-neighbor coordination shell the strongest interaction is between transition metal atoms, originating from *d*-electron "Friedel-like" bonding. This should be reflected as in the electronic structure of alloys as well as in specific parameters characterizing *d*-band.

In Fig. 6 we show the total density of states (DOS) and local DOS in the atomic sphere of Pd in Ag-Pd random alloys for eight different concentrations at the interval of 10 at. % of Pd. When the concentration of Pd is small, the *d*-electrons of Pd practically do not participate in the bonding forming an impuritylike state (bottom panel). The addition of Pd to the alloy gradually increases the overlapping of localized *d*-states, thereby increasing the width of the *d*-band and in its turn the interaction between Pd atoms. One can see, that a well developed *d*-band of Pd is formed at about 40–50 at. % of Pd. This composition is exactly the one where both V_1 and V_2 change their concentration behavior in Cu- and Ag-Pd alloys. This is also the composition where the enthalpy of mixing of random Ag-Pd alloys has a minimum.[72]

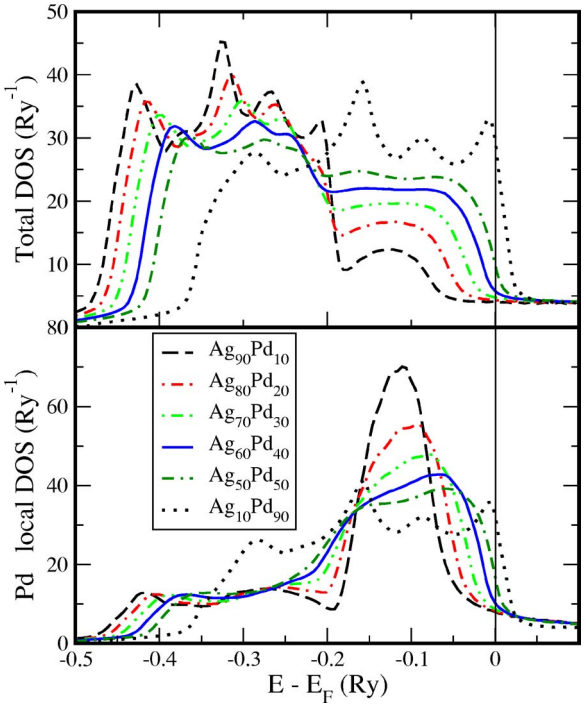

FIG. 6. (Color online) The total density of states (top panel) and local Pd DOS (lower panel) in Ag-Pd alloys.

We do not show the DOS in Ag-Pt alloys due to a very close similarity to that of Ag-Pd. The only difference is that in Pt alloys a formation of common *d*-band occurs at about 30–40 at. % due to a broader in energy and less spatially localized Pt *d*-states. This difference between Pd and Pt in Ag alloys can be clearly seen in Fig. 7 where on the upper panel we show the number of *d*-electrons in the atomic spheres of Pd and Pt and on the lower panel the *d*-band center positions (relative to the Fermi energy) as a function of Pd(Pt) concentration. The position of the center of the *d*-band, C_d is also an important band-structure parameter, which can be used for characterization of the bonding.[59,60] Although we do not have a model, which directly connects C_d with the effective interactions at different coordination shells, it is obvious that the concentration dependencies of C_d in Fig. 7 and V_2 in Fig. 5 are very similar.

A simplified connection between C_d and the interaction between transition metal atoms can be established using the formalism developed by Alexander-Anderson[61] and Heine[62] and adopted to the case of Green's function KKR method by Oswald *et al.*[63] and Hoshino *et al.*[60] They have shown that the interactions v between *d*-metal atoms, is given by the corresponding intersite Green's function, which should be inversely proportional to the position of *d*-band center, C_d, i.e., $v \sim \int dE \frac{1}{E-C_d-i\Gamma}$, where Γ is parameter related to the

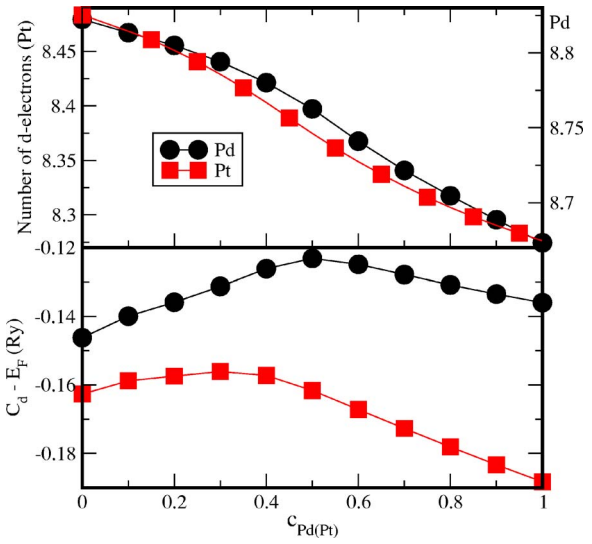

FIG. 7. (Color online) *d*-band parameters in Ag-Pd and Ag-Pt alloys. Top panel: Number of *d*-electrons in atomic sphere of Pd (the scale on the left-hand side) and Pt (the scale on the right-hand side). Bottom panel: Center of Pd and Pt *d*-band in Ag-Pd(Pt) alloys.

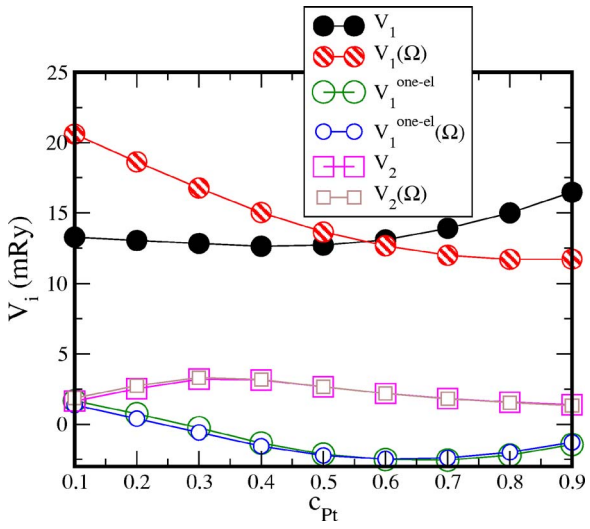

FIG. 8. (Color online) SGPM effective interaction in CuPt.

d-band width.[62] This means that a relative change of the interaction is approximately (in the lowest order) proportional to the *relative shift* of the *d*-band center, ΔC_d. This is very similar to the Hammer-Norskov model,[64] connecting the shift of the center of the *d*-band of a transition metal substrate with strength of the bonding of an adsorbate. This model is widely used in the theory of catalysis.[65,66]

Another important parameter is the number of *d*-electrons in the atomic sphere of transition metal atoms. One can see in Fig. 7 that the number of *d*-electrons in the Pd atomic sphere is greater than that in Pt. The more *d*-states there are in the atomic sphere, the stronger localization. With increasing Pd (Pt) concentration the overlap between Pd(Pt) *d*-states increases and less *d*-electrons remain localized in the atomic spheres. This can be also described as a $s-d$ charge transfer. That is, probably, why V_1 is monotonously decreasing with Pd (Pt) concentration: the more Pd or Pt there is in an alloy, the stronger *d*-band bonding, which is reflected, in accordance with the Friedel tight-binding model, in the decreasing number of *d*-electrons.

This is also the reason why V_1 in Pt alloys is substantially lower than that in Pd alloys: The bonding between Pt atoms is stronger than that between Pd atoms. This is a combined effect of broader *d*-band of Pt and less occupied *d*-states of Pt atoms (see Fig. 7). This explains why there exists a pronounced phase separation tendency in Ag-Pt and Au-Pt alloys, while Ag-Pd and Au-Pd alloys exhibit weak ordering. The simple arguments presented above have been demonstrated and explained by Hoshino *et al.*,[60] who calculated 3*d*- and 4*d*-impurity-impurity interactions in Cu and Ag for the first two coordination shells. They also reported a strong tendency towards phase separation in all the Ag-LTM alloys, where LTM stands for all the late transition metals having the number of *d*-electrons less than that in Pt and Pd. They ascribed this tendency to the strong attractive interactions between transition metal atoms.

C. Screened Coulomb interactions in Cu-Pt and Cu-Pd alloys

So far we have neglected the screened electrostatic interaction at the first coordination shell. As has been mentioned above it is quite small in all the considered alloys, except Cu-Pd and Cu-Pt. As can be seen from Fig. 8, where we show the fist two SGPM pair interactions in Cu-Pt as a function of Pt concentration, the screened electrostatic interaction gives the dominant positive contribution to the nearest-neighbor effective pair interaction. It actually originates from a substantial size difference between the Cu and Pd(Pt) atoms, leading to a large value of the effective charge transfer, q_{eff}. In other words, the screened Coulomb interaction provides a very strong attractive force between Cu and Pd (Pt) atoms at the first coordination shell, thus favoring alloying and ordering.

This contribution is absent in the case of Ag(Au)-Pt(Pd) alloys, so that other *interatomic* potentials become more important changing the alloying and ordering behavior. In particular, the phase-separation (or clustering, segregation) tendency in Ag-Pt and Au-Pt alloys is due to the relatively strong Pt-Pt interactions at the first coordination shell, as described above. We would like to point out that the contribution of the screened Coulomb interaction discussed here has exactly the same nature as the electrostatic interaction energy of two impurities derived using the Hellman-Feynman theorem by Klemradt *et al.*,[67] although the latter consider it as a *repulsion* of the atoms of the same type.

Let us now return to Fig. 8, where we show two sets of the SGPM pair interactions at the first and second coordination shells. The first set, which is shown without indicating dependence upon the volume, Ω, has been calculated at a fixed Wigner-Seitz radius of 2.75 a.u. The second set of interactions with volume dependence, $V_i(\Omega)$, has been calculated at different Wigner-Seitz radii, changing linearly with concentration from 2.72 a.u. for $Cu_{90}Pt_{10}$ to 2.83 a.u. for $Cu_{10}Pt_{90}$ alloys. We also show two sets of the one-electron part of the effective interaction at the first coordination shell, $V_1^{\text{one-el}}$, with and without volume dependence. It is clear that both $V_1^{\text{one-el}}$ and V_2, for which the screening contribution is

TABLE V. The energies of some ordered structures in terms of the first two effective pair interactions relative to the ordering energy of the $L1_0$ ($L1_2$) structure, which is $-c(1-c)(2V_1-3V_2)$.

	CH	$L1_1$	$L1_1^+$	V1
$\Delta E_{\mathrm{ord}}/c(1-c)$	$-2V_2$	$2(V_1-3V_2)$	$\frac{4}{3}(V_1-3V_2)$	$4V_1-4V_2$

small, are practically volume independent. In other words, the volume dependence of V_1 originates from the screened Coulomb interactions: The increase of volume with increasing concentration of Pt leads to a decrease of q_{eff} and V_1^{scr}. It is also clear that the strong ordering tendency in Cu-Pt is due to this electrostatic interaction, which makes V_1 large and positive. Similarly the strong ordering tendency in Cu-Pd compared to Ag-Pd is also due to electrostatic interactions between Cu and Pd at the first coordination shell.

D. Ordering trends from the first two pair interactions

As has been mentioned above, all the variety of ordering behavior, exhibited by the alloys isoelectronic to Ag-Pd, can be qualitatively understood using the results for the first two effective interactions only. In Table V we show the energies of the CH, $L1_1$, $L1_1^+$, and $V1$ structures relative to that of $L1_0$ ($L1_2$) (as has been discussed above, the energetics of the LPS is related to the long-range interactions due to the Fermi-surface-nesting effects) in terms of the first two pair interactions. If we use this simple estimate to find the most stable structure among the structures listed above, we get the results presented in Table VI.

As one can see we get correct answers in all cases, except $Au_{50}Pd_{50}$, which is stable in the CH structure, and $Cu_{50}Pt_{50}$, which is stable in the $L1_1$ structure. In those two cases more distant effective cluster interactions are responsible for the stabilization of the correct ground state structures. In particular Clark *et al.*[68] have demonstrated that a van Hove singularity is responsible for the $L1_1$ ordering in Cu-Pt and Au-Pt. Let us also notice that at variance with our results Sanyal *et al.*[69] have recently found that the first two GPM pair interactions stabilize the $L1_1$ structure of Cu-Pt. Their GPM calculations have been performed without screened electrostatic interactions by adjusting the atomic sphere radii of alloy components to make thier average net charges vanish.

Nevetheless, it is clear that using just the first two effective interactions we can explain practically all the ordering trends in the whole family of alloys isoelectronic to Ag-Pd. In particular, stabilization of the CH, $L1_1$, and $V1$ structures is a consequence of strong ordering (positive) interactions at the second coordination shell. This is the case in all the systems except Au-Pd, where V_2 is very small and becomes even negative in the case of $Au_{25}Pd_{75}$.

VI. SURFACE SEGREGATION IN Ag-Pd

The surface segregation in Ag-Pd alloys has been previously investigated using first-principles calculations by several authors, starting from the pioneering work by Abrikosov and Skriver,[30] followed by the work of Drchal *et al.*,[70] and the most recent work by Ropo *et al.*[71,72] In all these calculations strong segregation of Ag atoms to the surface is obtained, which is quite expected since Ag has much lower surface energy than Pd. Such segregation behavior has also been observed experimentally.[27,73] What makes this system quite interesting for a new theoretical investigation is the existence of the STM data for the (111) and (100) surfaces of $Ag_{33}Pd_{67}$.[27] The STM images allow one to observe *in situ* not only the surface alloy composition, but also the atomic configuration or short-range order.

The key quantity, which determines the surface segregation phenomenon, is the surface segregation energy, defined as the energy cost to transfer an atom of a certain type from bulk into the surface layer. In Table VII we show our results for the surface segregation energies of Ag for three different facets of homogeneous random Ag-Pd alloys. In all cases the

TABLE VI. The effective pair interactions (in mRy) at the first two coordination shells in Ag(Cu,Au)-Pd(Pt) alloys and the structure stabilzied by these interactions.

Alloy	V_1	V_2	Structure	Alloy	V_1	V_2	Structure
$Cu_{75}Pd_{25}$	8.91	0.60	$L1_2$	$Cu_{75}Pt_{25}$	15.19	3.02	$L1_2$
$Cu_{50}Pd_{50}$	7.57	1.53	CH	$Cu_{50}Pt_{50}$	12.71	2.66	CH
$Cu_{25}Pd_{75}$	5.73	0.33	$L1_2$	$Cu_{25}Pt_{75}$	11.76	1.66	$L1_2$
$Ag_{75}Pd_{25}$	2.12	0.83	$L1_2$	$Ag_{75}Pt_{25}$	−0.57	2.77	$V1$
$Ag_{50}Pd_{50}$	1.19	1.59	$L1_1$	$Ag_{50}Pt_{50}$	−2.57	2.67	$L1_1$
$Ag_{25}Pd_{75}$	−0.38	0.14	$V1$	$Ag_{25}Pt_{75}$	−3.15	1.43	$L1_1$
$Au_{75}Pd_{25}$	4.95	0.09	$L1_2$	$Au_{75}Pt_{25}$	−0.73	1.43	$V1$
$Au_{50}Pd_{50}$	3.98	−0.01	$L1_0$	$Au_{50}Pt_{50}$	−2.32	0.68	$L1_1$
$Au_{25}Pd_{75}$	2.93	−0.56	$L1_2$	$Au_{25}Pt_{75}$	−2.81	0.16	$V1$

TABLE VII. Surface segregation energy (in eV) of Ag for (111), (001), and (110) facets in homogeneous Ag-Pd alloys. The values of the corresponding surface energy differences of pure Ag and Pd are given in the parentheses.

Surface	Ag	$Ag_{75}Pd_{25}$	$Ag_{50}Pd_{50}$	$Ag_{33}Pd_{67}$	Pd
fcc(111)	−0.20 (−0.27)	−0.23	−0.24	−0.25	−0.31 (−0.33)
fcc(100)	−0.40 (−0.37)	−0.38	−0.35	−0.34	−0.42 (−0.44)
fcc(110)	−0.52 (−0.54)	−0.49	−0.44	−0.45	−0.53 (−0.63)

experimental lattice spacing has been used in the calculations. The results for pure Ag and Pd have been obtained in the LSGF calculations of a single impurity in the bulk and in the surface layer. We have used three different supercells of size $6\times6\times15$, $6\times6\times16$ and $4\times8\times24$ for the fcc(111), fcc(100), and fcc(110) surfaces, respectively, with five vacuum layers in the case of fcc(111) and fcc(100) surfaces, and nine vacuum layers for the fcc(110) surface. The surface segregation energies in the random homogeneous alloys have been obtained by means of the surface Green's function techniques,[31] with the chemical potentials obtained from the corresponding bulk KKR-ASA(+M) calculations. The on-site screening constants in all the layers have been fixed to the corresponding bulk values. The latter is, of course, an approximation. However charge transfer effects play a minor role in the energetics of Ag-Pd alloys.

A. Surface segregation energies and effective pair interactions

As one can see from Table VII the concentration dependence of the surface segregation energy is rather weak, and partly this is a volume effect. The latter can be seen from the surface energy difference of pure Ag and Pd given in Table VII in parentheses, which are calculated at the corresponding lattice spacing of Ag and Pd. The increasing surface segregation tendency for more open surfaces is due to the fact that surface energies are proportional to the "number of broken bonds,"[74,75] so the difference between the surface energies of Ag and Pd is also increasing with reducing coordination number of the surface atoms. A relatively weak dependence of the surface segregation energy on the surface alloy composition has been demonstrated by Ropo *et al.*[72]

Let us notice that the results in Table VII are slightly different from those presented in Ref. 76 and Ref. 71, where the surface segregation energy for the (111) surface is found to be −0.26 and −0.28 eV, respectively. The difference from the results of Ref. 76 comes from the fact that in Ref. 76 the equilibrium LDA theoretical volume has been used, which is slightly lower than the experimental one. Nevertheless the overall conclusion is clear: The surface layer in AgPd alloys should be strongly enriched by Ag, especially in the case of more open surfaces.

In contrast to the surface segregation energies the effective pair and multisite interactions on the surface of alloys exhibit a nonlinear concentration dependence similar to the case of bulk alloys. Moreover they are concentration-profile dependent. To demonstrate such a dependence we show in Fig. 9 the values of the nearest neighbor effective pair interactions in the first, $V_{1\text{-}1;1}$, and second layers, $V_{2\text{-}2;1}$, as well as between the first and second layers, $V_{1\text{-}2;1}$, as a function of the Pd concentration in the *second* layer for the fcc(111) surface of $Ag_{50}Pd_{50}$. The composition in the first layer has been fixed to $Ag_{90}Pd_{10}$. One can also notice that, although the composition of the surface layer is fixed, the value of the effective pair interaction in this layer depends strongly on the concentration in the next, subsurface layer.

Such a complicated concentration dependence of the cluster interactions on the concentrations is very difficult to model using a concentration-independent cluster expansion. In Monte Carlo (MC) calculations of the surface concentration profiles we redetermined the effective cluster interactions in accordance with the current values of the concentrations during simulations. The on-site interactions were kept fixed because, as has been discussed above, they turned out to be very little dependent on the alloy composition near the surface. We also restricted the number of interactions included in the MC calculations: Only the first 10 effective pair interactions and one 3-site interaction of the triangle of the nearest neighbors have been considered. This is an acceptable model since we do not consider any ordering phase transitions or related effects.

In the case of Ag-Pd it is actually extremely difficult and cumbersome to consider all the interactions needed for the quantitatively correct description of ordering near the surface at 0 K, especially for the Ag-rich alloys, where the LPS are stabilized by long-range interactions. In the case of surface alloys the number of interactions grows dramatically due to

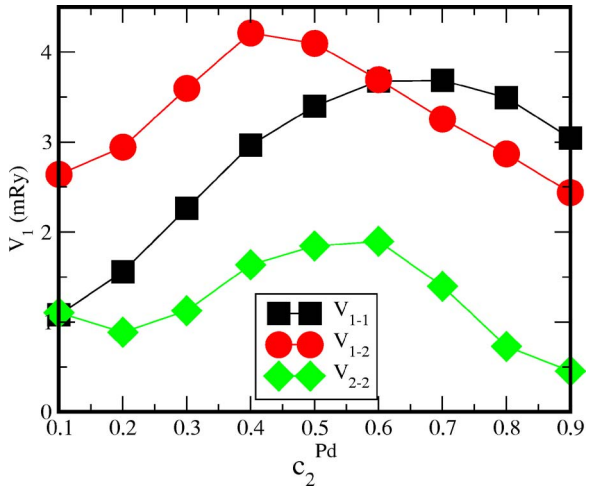

FIG. 9. (Color online) In-plane surface, $V_{1\text{-}1}$, interplane surface-subsurface, $V_{1\text{-}2}$, and in-plane subsurface, $V_{2\text{-}2}$, SGPM effective interactions on the first coordination shell for fcc(111) $Ag_{50}Pd_{50}$ alloy, as a function of the Pd concentration in the subsurface layer. The composition of the surface layer is is fixed to be $Ag_{90}Pd_{10}$.

TABLE VIII. Ag concentration in the fist four layer of $Ag_{75}Pd_{25}$, $Ag_{50}Pd_{50}$, and $Ag_{33}Pd_{67}$ alloys on (111) and (001) surfaces at 800 K. The results by Ropo *et al.* (Refs. 71 and 72) are given in parentheses. Experimental data from Ref. 27.

Surface	Layer	$Ag_{75}Pd_{25}$	$Ag_{50}Pd_{50}$	$Ag_{33}Pd_{67}$	$Ag_{33}Pd_{67}$-expt.
fcc(111)	1	0.99	0.85 (0.85)	0.88	0.95
	2	0.77	0.40 (0.39)	0.25	
	3	0.77	0.54	0.53	
	4	0.74	0.49	0.33	
fcc(100)	1	1.00	0.98	0.98	1.0
	2	0.65	0.32	0.22	
	3	0.82	0.41	0.24	
	4	0.73	0.52	0.34	

their layer and position dependence. Besides, the inclusion of long-range layer-dependent interactions leads to a growth of the number of nonequivalent or "surface" layers in the setup for the Monte Carlo simulation box. At the same time, the main purpose of these simulations is to find the high-temperature concentration profile. In the bulk Monte Carlo simulations, which were performed with the whole set of interactions, we have found the ordering phase transitions at about room temperature, very similar to the results by Müller and Zunger.[25] These very weak ordering effects connected with long-range interactions can be safely neglected at temperatures above 700 K.

B. Results of statistical thermodynamic simulations

The results of our calculations for three different alloy compositions, $Ag_{75}Pd_{25}$, $Ag_{50}Pd_{50}$, and $Ag_{33}Pd_{67}$ and for two different facets, (111) and (001), of the fcc lattice at 800 K are presented in Table VIII. In all the cases we find very strong segregation of Ag atoms toward the surface. The (001) is almost entirely covered with Ag atoms, which is in agreement with the experimental data of Wouda *et al.*[27] More pronounced segregation of Ag on the more open (001) surface, than on the close-packed (111) surface, is the result of the increased segregation tendency as was explained above. One can also notice that in all cases except $Ag_{75}Pd_{25}(111)$ the second layer is enriched with Pd. This is an ordering effect.

As a matter of fact the segregation energy of Ag into the second layer of the (111) surfaces is also *negative* although rather small, about −0.05 eV. Therefore the second layer in these alloys should also be enriched by Ag in the absence of ordering effects. However the strong surface segregation of Ag and the ordering interaction at the *second* coordination shell, lead to the Pd enrichment of the second layer. This is exactly the type of ordering behavior which has been observed in the case of bulk Ag-Pd alloys when the pair interaction at the second coordination shell becomes dominant close to the equiatomic alloy composition (see Fig. 5). This also explains why there is no such effect in the case of $Ag_{75}Pd_{25}(111)$: The interaction at the second coordination shell is simply not strong enough for this alloy composition.

In this respect, very good agreement between our results and results by Ropo *et al.*[72] might seem puzzling, since Ropo *et al.* have performed only single-site mean-field calculations, based on the minimization of the energy of random inhomogeneous surface alloys. However, in fact, such calculations indeed capture the interlayer ordering tendency correctly. They completely neglect the *intralayer* ordering, but this is not needed in the high-temperature consideration, far above order-disorder phase transition where the short-range order (SRO) effects are small and cannot influence the layer composition.

The calculated surface composition of $Ag_{33}Pd_{67}(111)$ is 88 at. % of Ag, which is in fair agreement with the STM experimental data by Wouda *et al.*,[27] who found 95 at. % of Ag at 820 K. The small difference can be due to theoretical approximations (neglect of lattice vibrations, relaxations, different types of errors, etc.) as well as due to the fact that the actual STM measurements have been done at low temperature and, although the bulk diffusion is practically suppressed, some atomic rearrangements are still possible near the surface during cooling from high temperatures.

Another piece of experimental information, which is consistent with our results, is the ordering type of the SRO for the first coordination shell on the surface. In particular, the Warren-Cowley SRO parameter[77] in our calculations is about −0.04, which indicates a pronounced ordering (the minimal value of the SRO for the surface layer is about −0.13). The effective interactions at the first coordination shell in the surface layer is 3.04 mRy for the concentration profile at 800 K, i.e., of ordering type. This is due to the Ag enrichment of the surface layer, otherwise clustering behavior would be found: The value of the nearest-neighbor effective pair interaction for the homogeneous surface concentration profile in $Ag_{33}Pd_{67}(111)$ is −0.74 mRy.

VII. CONCLUSIONS

The SGPM has allowed us to illuminate the origin of similarities and differences in the ordering behavior in Ag-Pd and isolelectronic alloys, as well as to explain systematic failures of the SIM-type approaches (based on the total energy calculations of a predefined set of ordered structures) to predict the LPS in the case of Ag-Pd and Au-Pd systems. Of course, it is very unlikely that any of these ordered structures will ever be formed in Ag-Pd alloys due to the very small

values of the ordering energies and low order-disorder transition temperatures. Nevertheless, the ordering behavior in Ag-Pd can be partly observed for alloy surfaces: Although the segregation is overwhelmingly governed by the segregation energies, there are ceritain features, like the short-range order in the layer or oscillating concentration profile, which are entirely due to specific ordering in the system.

We have demonstrated that the tendency towards formation of the LPS is a common feature in the Pd(Pt)-deficient region of the Ag-Pd isolelectronic alloys. The formation of the LPS in the case of Ag(Au)-Pt is, however, hampered by the strong Pt-Pt interactions, which substantially reduce the effective interaction at the first coordination shell, making it *negative*, and thereby completely destabilize the $L1_2$-type of ordering. This does not happen in the case of Cu-Pt system, since, the interaction between Cu and Pt atoms at the first coordination shell is strongly attractive due to the screened Coulomb interactions.

Another common feature in the ordering behavior of alloys isoelectronic to Ag-Pd is the tendency toward formation of (111)-type ordered structures, like $L1_1$ ($L1_1^+$, CH, or $V1$). The tendency originates from a relatively strong ordering interactions at the second coordination shell, i.e., large and positive values of V_2. It is especially pronounced in the case of Cu-Pt and Ag-Pt alloys. In Pd-rich Ag-Pd alloys this type of ordering leads to oscillating concentration profiles for the (111) surfaces.

ACKNOWLEDGMENTS

The authors are grateful to The Swedish Research Council (VR) and the Swedish Foundation for Strategic Research (SSF) for financial support. Most of the simulations were carried out at the Swedish National Infrastructure for Computing (SNIC).

[1] D. de Fontaine, Solid State Phys. **34**, 73 (1979).
[2] A. Khachaturyan, *Theory of Structural Transformations in Solids* (Wiley, New York, 1983).
[3] F. Ducastelle, *Order and Phase Stability in Alloys* (North-Holland, Amsterdam, 1991).
[4] J. M. Sanchez, F. Ducastelle, and D. Gratias, Physica A **128**, 334 (1984).
[5] A. van de Walle and G. Ceder, J. Phase Equilib. **23**, 348 (2002).
[6] N. A. Zarkevich and D. D. Johnson, Phys. Rev. Lett. **92**, 255702 (2004).
[7] V. Blum, G. L. W. Hart, M. J. Walorski, and A. Zunger, Phys. Rev. B **72**, 165113 (2005).
[8] S. V. Barabash, V. Blum, S. Müller, and A. Zunger, Phys. Rev. B **74**, 035108 (2006).
[9] G. Trimarchi, P. Graf, and A. Zunger, Phys. Rev. B **74**, 014204 (2006).
[10] A. V. Ruban, S. Shallcross, S. I. Simak, and H. L. Skriver, Phys. Rev. B **70**, 125115 (2004).
[11] F. Ducastelle and F. Gautier, J. Phys. F: Met. Phys. **6**, 2039 (1976).
[12] P. E. A. Turchi, G. M. Stocks, W. H. Butler, D. M. Nicholson, and A. Gonis, Phys. Rev. B **37**, 5982 (1988).
[13] B. L. Györffy and G. M. Stocks, Phys. Rev. Lett. **50**, 374 (1983).
[14] J. B. Staunton, D. D. Johnson, and F. J. Pinski, Phys. Rev. B **50**, 1450 (1994).
[15] J. W. D. Connolly and A. R. Williams, Phys. Rev. B **27**, 5169 (1983).
[16] A. Zunger, in *Statics and Dynamics of Alloy Phase Transformations*, edited by P. Turchi and A. Gonis. NATO Advanced Study Institute Series (Plenum, New York, 1994), p. 361.
[17] V. Drchal, J. Kudrnovský, L. Udvardi, P. Weinberger, and A. Pasturel, Phys. Rev. B **45**, 14328 (1992).
[18] R. Monnier, Philos. Mag. B **75**, 67 (1997).
[19] A. V. Ruban and H. L. Skriver, Phys. Rev. B **55**, 8801 (1997).
[20] A. V. Ruban and H. L. Skriver, Phys. Rev. B **66**, 024201 (2002).
[21] A. V. Ruban, S. I. Simak, P. A. Korzhavyi, and H. L. Skriver, Phys. Rev. B **66**, 024202 (2002).
[22] L. V. Pourovskii, A. V. Ruban, B. Johansson, and I. A. Abrikosov, Phys. Rev. Lett. **90**, 026105 (2003).
[23] *Binary Alloy Phase Diagrams*, edited by T. B. Massalski (ASM International, Metals Park, OH, 1992).
[24] Z. W. Lu, S.-H. Wei, A. Zunger, S. Frota-Pessoa, and L. G. Ferreira, Phys. Rev. B **44**, 512 (1991).
[25] S. Müller and A. Zunger, Phys. Rev. Lett. **87**, 165502 (2001).
[26] S. Curtarolo, D. Morgan, and G. Ceder, CALPHAD: Comput. Coupling Phase Diagrams Thermochem. **29**, 163 (2005).
[27] P. T. Wouda, M. Schmid, B. E. Nieuwenhuys, and P. Varga, Surf. Sci. **417**, 292 (1998).
[28] J. Korringa, Physica (Amsterdam) **13**, 392 (1947); W. Kohn and N. Rostoker, Phys. Rev. **94**, 1111 (1954).
[29] O. Gunnarsson, O. Jepsen, and O. K. Andersen, Phys. Rev. B **27**, 7144 (1983).
[30] I. A. Abrikosov and H. L. Skriver, Phys. Rev. B **47**, 16532 (1993).
[31] A. V. Ruban and H. L. Skriver, Comput. Mater. Sci. **15**, 119 (1999).
[32] P. E. Blöchl, Phys. Rev. B **50**, 17953 (1994).
[33] G. Kresse and D. Joubert, Phys. Rev. B **59**, 1758 (1999).
[34] G. Kresse and J. Hafner, Phys. Rev. B **48**, 13115 (1993).
[35] G. Kresse and J. Furthmüller, Comput. Mater. Sci. **6**, 15 (1996); Phys. Rev. B **54**, 11169 (1996).
[36] D. D. Johnson, D. M. Nicholson, F. J. Pinski, B. L. Gyorffy, and G. M. Stocks, Phys. Rev. B **41**, 9701 (1990).
[37] J. P. Perdew and Y. Wang, Phys. Rev. B **45**, 13244 (1992).
[38] H. J. Monkhorst and J. D. Pack, Phys. Rev. B **13**, 5188 (1972).
[39] I. A. Abrikosov, A. M. N. Niklasson, S. I. Simak, B. Johansson, A. V. Ruban, and H. L. Skriver, Phys. Rev. Lett. **76**, 4203 (1996).
[40] I. A. Abrikosov, S. I. Simak, B. Johansson, A. V. Ruban, and H. L. Skriver, Phys. Rev. B **56**, 9319 (1997).
[41] Note that in the earlier heuristic models for screening, like the screened impurity model (Ref. 42) or the scr-CPA (Ref. 43) it is assumed that the screening charge is located at the nearest-neighbor sites around the impurity. In such a case α_{scr} depen-

dends only on the underlying crystal structure. For instance, for the fcc structure one gets $\alpha_{scr}=0.552\,669\,00$.

[42] I. A. Abrikosov, Yu. H. Vekilov, P. A. Korzhavyi, A. V. Ruban, and L. E. Shilkrot, Solid State Commun. **83**, 867 (1992).

[43] D. D. Johnson and F. J. Pinski, Phys. Rev. B **48**, 11553 (1993).

[44] N. Metropolis, A. W. Rosenbluth, M. N. Rosenbluth, A. H. Teller, and E. Teller, J. Chem. Phys. **21**, 1087 (1953).

[45] L. V. Pourovskii, A. V. Ruban, I. A. Abrikosov, Y. Kh. Vekilov, and B. Johansson, Phys. Rev. B **64**, 035421 (2001).

[46] D. K. Saha, K. Koga, and K. Ohshima, J. Phys.: Condens. Matter **4**, 10093 (1992).

[47] D. K. Saha and K. Ohshima, J. Phys.: Condens. Matter **5**, 4099 (1993).

[48] M. A. Krivogalz, *Diffuse Scattering of X-rays and Neutrons by Fluctuations* (Springer, Berlin, 1996).

[49] S. C. Moss and R. H. Walker, J. Appl. Crystallogr. **8**, 96 (1975).

[50] I. Wilkinson, R. J. Hughes, Z. Major, S. B. Dugdale, M. A. Alam, E. Bruno, B. Ginatempo, and E. S. Giuliano, Phys. Rev. Lett. **87**, 216401 (2001).

[51] I. Tsatskis, in *Local Structure from Diffraction*, edited by S. G. L. Billinge and M. F. Thorpe (Plenum, New York, 1998), p. 208.

[52] V. Ozolins, C. Wolverton, and A. Zunger Phys. Rev. Lett. **79**, 955 (1997); H. Reichert, S. C. Moss, and K. S. Liang, *ibid.* **79**, 956 (1997).

[53] S. C. Moss and H. Reichert, *Local Structure from Diffraction*, edited by S. G. L. Billinge and M. F. Thorpe (Plenum, New York, 1998), p. 189.

[54] Ph. Durussel and P. Feschotte, J. Alloys Compd. **239**, 226 (1996).

[55] M. H. F. Sluiter, C. Colinet, and A. Pasturel, Phys. Rev. B **73**, 174204 (2006).

[56] D. D. Johnson, A. V. Smirnov, J. B. Staunton, F. J. Pinski, and W. A. Shelton, Phys. Rev. B **62**, R11917 (2000).

[57] In the case of Au_3Pd the answer depends on exchange-correlation functional used in the calculations. For the LDA lattice parameter of 4.01 Å, which is sligtly smaller than the experimental one, 4.03 Å, the DO_{23} structure is practically degenerated in energy with the LPS3. At the experimental lattice spacing the LPS3 is marginally stable (actually the GGA increases the stability of the LPS3 in this case, on a fixed lattice spacing). At the GGA equilibrium lattice parameter, 4.12 Å, which is larger than the experimental one, the LPS3 is lower in energy than the DO_{23} structure by about 0.6 meV. Let us note that such a volume dependence of the ordering energy for the LPS can be observed as a temperature dependence of the position of the peak in diffuse scattering experiments due to the thermal lattice expansion.

[58] S. Takizawa, S. Blügel, K. Terakura, and T. Oguchi, Phys. Rev. B **43**, 947 (1991).

[59] D. G. Pettifor, *Bonding and Structure of Molecules and Solids* (Clarendon, Oxford, 1995).

[60] T. Hoshino, W. Schweika, R. Zeller, and P. H. Dederichs, Phys. Rev. B **47**, 5106 (1993).

[61] S. Alexander and P. W. Anderson, Phys. Rev. **133**, A1594 (1964).

[62] V. Heine, Phys. Rev. **153**, 673 (1967).

[63] A. Oswald, R. Zeller, P. J. Branspanning, and P. H. Dederichs, J. Phys. F: Met. Phys. **15**, 193 (1985).

[64] B. Hammer and J. K. Norskov, Surf. Sci. **343**, 211 (1995).

[65] J. Greely, J. K. Norskov, and M. Mavrikakis, Annu. Rev. Phys. Chem. **53**, 319 (2002).

[66] Y. Xu, A. V. Ruban, and M. Mavrikakis, J. Am. Chem. Soc. **126**, 4714 (2004).

[67] U. Klemradt, B. Drittler, R. Zeller, and P. H. Dederichs, Phys. Rev. Lett. **64**, 2803 (1990); U. Klemradt, B. Drittler, T. Hoshino, R. Zeller, P. H. Dederichs, and N. Stefanou, Phys. Rev. B **43**, 9487 (1991).

[68] J. F. Clark, F. J. Pinski, D. D. Johnson, P. A. Sterne, J. B. Staunton, and B. Ginatempo, Phys. Rev. Lett. **74**, 3225 (1995).

[69] B. Sanyal, S. K. Bose, V. Drchal, and J. Kudrnovsky, Phys. Rev. B **64**, 134111 (2001).

[70] V. Drchal, A. Pasturel, R. Monnier, J. Kudrnovsky, and P. Weinberger, Comput. Mater. Sci. **15**, 144 (1999).

[71] M. Ropo, K. Kokko, L. Vitos, and J. Kollar, Phys. Rev. B **71**, 045411 (2005).

[72] M. Ropo, K. Kokko, L. Vitos, J. Kollar, and B. Johansson, Surf. Sci. **600**, 904 (2006).

[73] F. Reniers, Surf. Interface Anal. **23**, 374 (1995).

[74] L. Vitos, A. V. Ruban, H. L. Skriver, and J. Kollar, Philos. Mag. B **78**, 487 (1998).

[75] I. Galanakis, G. Bihlmayer, V. Bellini, N. Papanikolaou, R. Zeller, S. Blügel, and P. H. Dederichs, Europhys. Lett. **58**, 751 (2002).

[76] A. V. Ruban, H. L. Skriver, and J. K. Norskov, Phys. Rev. B **59**, 15990 (1999).

[77] It is defined in terms of concentration variables, $c_i=1/2(\sigma_i+1)$, as $\alpha_p=\frac{\langle c_i c_j\rangle_p - c^2}{c(1-c)}$, where sites i and j belong to the pth coordination shell.